PRINCESS MÁXIMA CENTER FOR PEDIATRIC ONCOLOGY

Identification of effective compounds in ATRX aberrant neuroblastoma cell lines

Final report major research project

Romy van Oosterhout

02-2022

Identification of effective compounds in ATRX aberrant neuroblastoma cell lines

Details

Version
1

Student
Romy van Oosterhout
6912451
w.m.vanoosterhout@students.uu.nl

Supervisors
Dr. Marlinde van den Boogaard
Michael van Gerven, PhD

Examiner
Prof. Dr. Jan Molenaar

Second reviewer
Dr. Marcel Kool

Date
15-02-2022

Location
Princess Máxima Center for Pediatric Oncology, Molenaar lab, Heidelberglaan 25, 3584 CS Utrecht, Netherlands

Education

Master Drug Innovation
Graduate School of Life Sciences
Utrecht University

Table of Contents

Layman's summary – Samenvatting voor leken

Neuroblastoom is een tumor die waarschijnlijk ontstaat vanuit voorloper cellen van het sympathische zenuwstelsel. Jaarlijks krijgen ongeveer 30 kinderen in Nederland de diagnose neuroblastoom, waarbij de meeste kinderen jonger zijn dan zes jaar. De tumor komt voornamelijk voor in de bijnieren, maar kan ook ontstaan in de buik, borstholte, hals of het bekken. Bij de diagnose wordt aan de hand van het genetische profiel, de plaats en eventuele uitzaaiingen de risico groep bepaald. Patiënten die in de lage- en gemiddelde risicogroep vallen hebben een overlevingskans van ongeveer 90 tot 100%, terwijl patiënten in de hoge risicogroep een overlevingskans van minder dan 50% laten zien, ondanks intensieve therapie. Een afwijking in het ATRX-gen is een indicatie voor het plaatsen van de patiënt in de hoge risicogroep. De meeste van deze afwijkingen betreffen deleties van hele exonen. Het ATRX-eiwit is onder andere betrokken bij het reguleren van genexpressie en stabiliteit van DNA doordat het de structuur van chromatine kan veranderen. Tevens wordt er in studies voorgesteld dat het ATRX-eiwit ook een rol speelt in het oplossen van secundaire DNA structuren genaamd G-quadruplexen (G4) om replicatie stress te voorkomen. Deze structuren zijn rijk aan guanine en hebben de neiging om het DNA replicatie proces te onderbreken waarbij DNA schade ontstaat. Wanneer er in kankercellen ATRX-mutaties optreden worden er meer G4 complexen teruggevonden, wat leidt tot meer DNA schade in deze cellen. Op dit moment zijn er beperkte therapieën beschikbaar voor neuroblastoom patiënten met een ATRX-afwijking. In de afgelopen jaren zijn er een aantal nieuwe therapie opties gevonden voor deze specifieke groep, maar deze therapieën bleken niet erg effectief te zijn in ons lab. Hierdoor is het doel van dit project om specifieke en efficiënte compounds te identificeren voor de behandeling van ATRX neuroblastoom patiënten. In het verleden zijn modellen van de meest voorkomende ATRX deleties in patiënten nagemaakt in neuroblastoom cellen, zodat de gevoeligheid voor compounds vergeleken kan worden met neuroblastoom cellen die geen ATRX-deletie hebben. In deze studie hebben we eerst 199 compounds getest op neuroblastoom cellen met en zonder een ATRX-afwijking. Hierin vonden we vijf compounds die een resistentie lieten zien in ATRX modellen tegenover cellen met een normale ATRX status. Twee van deze compounds worden momenteel ook in de kliniek gebruikt voor de behandeling van neuroblastoom. Echter waren we opzoek naar compounds die juist gevoeliger werden in ATRX modellen. Nadat we geen specifieke compound voor ATRX konden identificeren, hebben we 12 compounds geselecteerd die aangrijpen op mechanismen waarvan bekend is dat ze veranderd zijn in neuroblastoom cellen met een ATRX-afwijking. Helaas vonden we ook hier geen specifieke compound voor ATRX, maar konden we wel drie compounds identificeren die effectief waren in alle geteste neuroblastoom cellen. Het combineren van compounds is gebruikelijk in de behandeling van kanker, waardoor we twee compounds hebben getest in combinatie met ruim 200 compounds. Echter bleek dit niet genoeg voor een krachtige combinatie. Hieruit kunnen we concluderen dat we in deze studie drie compounds hebben gevonden die mogelijk interessant zijn voor de behandeling van neuroblastoom.

Abstract

Neuroblastoma is the most common extracranial solid tumour among children that originates from undifferentiated neural crest cells. Despite intensive therapy, high-risk disease patients still show a poor overall survival rate. Within the high-risk neuroblastomas, ~15% of the patients have an aberration in the chromatin remodeller ATRX. Most of these aberrations are large in-frame exon deletions that still result in a protein product. ATRX is highly enriched at GC-rich regions where it deposits histones and is suggested to resolve G-quadruplex structures to maintain genomic stability. Currently, there are limited therapy options available for patients with ATRX aberrant neuroblastoma. These proposed therapies have not passed clinical trials so far, and therefore there is an urgent need for new effective therapies for children with high-risk neuroblastoma. Here, we performed high-throughput drug screens to identify potential compounds that target ATRX aberrant cells. Using patient-derived and isogenic ATRX models, we found three compounds that are effective in multiple neuroblastoma lines, independently of TP53 and 11q status. Additionally, we identified that ATRX 2-10 deletion models were less sensitive for five compounds. Four of these compounds target cell proliferation. We show that three compounds (Pidnarulex, BMH-21 and NSC 617145) are not ATRX specific, but might be of interest for neuroblastoma therapy in general.

1. Introduction

Neuroblastoma is a solid tumour of the peripheral sympathetic nervous system that is most common in infants and is rarely seen in children over five years old[1,2]. Each year, 7-12 new cases of neuroblastoma per million children are identified worldwide, with higher rates in the first year of life[3]. It is a type of tumour that is typically located in the abdomen, most commonly in the adrenal medulla and sympathetic ganglia[4]. Neuroblastoma is assumed to originate from primordial neural crest cells during development[5]. These precursor cells are involved in the development of the sympathetic nervous system and do not differentiate normally, rather they continue to proliferate and migrate in an immature state, forming tumours that press on nearby organs or cause metastasis[6]. In addition, intratumor heterogeneity is an important hallmark of neuroblastoma[7]. While patients with low- and intermediate risk disease have a survival rate of 90-100%, those with high-risk disease show an overall survival of less than 50% despite intensive therapy[8,9].

The three most common genetic alterations in high-risk neuroblastoma are MYCN amplifications, telomerase reverse transcriptase (TERT) rearrangements, and α-thalassaemia mental retardation X-linked (ATRX) abberations[10]. In older patients with stage 4 neuroblastoma, ATRX aberrations are more commonly identified. These patients are associated with poor prognosis and lack of effective therapies[11–13]. Both ATRX point mutations and whole exon deletions have been identified in the last decade, but large deletions (~70%) are more common and almost exclusively present in neuroblastoma (Unpublished meta-analysis, van Gerven *et al.*). These types of deletions are predicted to be in-frame (IFD) and still generate a shorter in-frame fusion (IFF) protein product (Unpublished meta-analysis, van Gerven *et al.*)[14].

ATRX is a SWI/SNF2 chromatin remodeller located on the X-chromosome. It is highly enriched at GC-rich and repetitive sequences where it regulates transcription[15,16]. ATRX interacts with the death-domain associated protein (DAXX) to maintain genomic stability through deposition of the histone variant H3.3 at both telomeric and pericentromeric regions[17]. Studies have hypothesised that ATRX, among its various functions, is involved in resolving G-quadruplexes (G4) to prevent replication stress[18–20]. These secondary structures tend to stall DNA replication fork progression, resulting in replication fork collapse that generates DNA damage[21]. Increased G4 formation has been observed in glioma cells with ATRX loss and this is linked to increased sensitivity to compounds that stabilize G4 structures[19]. Consistent with increased DNA damage as a result of more G4 structures, ATRX loss indirectly affects the DNA damage response (DDR) pathway[22]. ATRX is recruited to sites of DNA damage and binds the replication fork complex MRE11, RAD50, NBS1 (MRN), which can degrade stalled forks[23]. ATRX loss is also strongly associated with, but not sufficient for the induction of Alternative Lengthening of Telomeres (ALT), a homologous recombination-based mechanisms utilised by 5-15% of cancer cells to maintain their telomeres[24]. The direct and indirect role of ATRX in the DDR response suggests that targeting these processes with selective compounds may be effective treatment options.

Currently, minimal therapy options that still need clinical validation are available for patients with ATRX aberrant neuroblastoma. One of these options includes PARP inhibitors, alone and in combination with a topoisomerase 1 (TOP1) inhibitor. They showed to be effective in an ATRX deleted neuroblastoma model[13]. However, in our preliminary data we did observe such a shift in sensitivity *in vitro* in our ATRX mutant line (CHLA90). Another identified potential therapy for ATRX IFF in neuroblastoma is the inhibition of ATRX's binding partner enhancer of zeste homolog 2 (EZH2), a histone methylating enzyme. In this study, they see an increased expression of REST in their ATRX IFF model, which sensitizes EZH2 for inhibition[14]. In our ATRX models we did not observe significant expression of REST, but screens with the EZH2 inhibitor are currently ongoing in our lab. WEE1 was

also found as a potential hit and WEE1 inhibition showed differences in sensitivity between WT and ATRX knock out cells[25,26], but we did not find this difference in our patient derived neuroblastoma lines. In another study, ATRX mutants were found to have a preferential sensitivity to ataxia telangiectasia mutated (ATM) inhibition in glioma and neuroblastoma cells[13,27]. We tested two ATM inhibitors on our models, however, we could not confirm this theory of preferential sensitivity in neuroblastoma ATRX deletion cells. This indicates that potential therapy options are limited, and therefore, there is an urgent need for new effective therapies for children with high-risk neuroblastoma.

In this study we aim to identify potential new therapies for ATRX aberrant neuroblastoma tumours. We used high-throughput screening with 199 compounds and manually selected twelve compounds targeting G4s and the DDR in order to identify an ATRX specific target. Although we did not find an ATRX specific compound, three compounds showed potential in all tested neuroblastoma models. To enhance efficacy and address tumour heterogeneity, combination therapy with compounds of different molecular targets are essential for treatment of cancer. Therefore, we performed combination screens with two out of the three identified compounds.

2. Materials and Methods

2.1. Reagents and drugs

Powdered BMH-21 (HY-12484, Bio-Connect), NSC 617145 (SML1005, Sigma-Aldrich), CX-5461 (Pidnarulex; HY-13323, Bio-Connect), CX-3543 (Quarfloxin; HY-14776, Bio-Connect), and X5050 (5.06026, Sigma-Aldrich) were dissolved in dimethylsuphoxide (DMSO) to make stock solutions with concentrations of 10 mM, 11.07 mM, 6.6 mM, 10.2 mM, and 10 mM and subsequently stored at -80°C. BRCA1-IN-2 (compound 15; HY-100862), D-I03 (HY-124691), (Z)-Mirin (HY-19959), ML216 (CID-4985229, HY-12342), Prexasertib (LY2606368; HY-18174), RI-2 (HY-16904), and Tazemetostat (EPZ-6438, E-7438; HY-13803) in DMSO with stock concentrations of 10 mM were purchased from Bio-Connect and stored at -20°C and -80°C.

2.2. Cell lines and culture conditions

Cell lines and organoids were grown in different types of media (Table S1). The cells were grown in a Forma Series 3 Water Jacketed CO_2 incubator (model 4121, Thermo Fisher Scientific) with 5% CO_2 and ~20% O_2 concentration at 37°C. All cells were tested for mycoplasma infections every six weeks and their identity was regularly validated through short tandem repeat profiling.

2.3. Cell viability assay for single and combination drug screens

For single compound testing, cells were counted by using a TC20 automated cell counter (1450102, Bio-Rad) and seeded in quadruplicate in 384-well plates (flat clear bottom black polystyrene tissue culture-treated microplates with lid, 3764, Corning) with at a density of 200 to 5000 cells per well (Table S3) with the Multidrop Combi Reagent Dispenser (5840300, Thermo Fisher Scientific). The cells were given 16-24 hours to attach, followed by treatment with the compounds using a five-fold series dilution ranging from from 5.12 pM to 2 µM for Prexasertib and 128 pM to 50 µM for the other 11 compounds using the D300e Digital Dispenser (Tecan). For combination testing, 1200 to 1500 cells per well (Table S3, AMC772T2 and CHLA90) were seeded in duplicates in 384-well plates. After 24 hours, the first set of compounds was added, followed by incubation of 72 hours at standard culturing conditions (5% CO_2, 37°C). The second set of compounds was added in a matrix of five-fold concentrations ranging from 25.6 pM to 10 µM, which were incubated for another 72 hours. In both single- and combination screens, cell viability was determined 72 h and/or 144 h after continuous exposure to drug by addition of 5 µL 3-(4,5-dimethylthiazol-2-yl)-2,5-diphenyltetrazoliumbromide (MTT, M2128, Sigma-Aldrich) solution (5 mg/mL MTT in sterile DPBS (14190250, Gibco, Thermo Fisher)) per well at standard culturing conditions. After 4 hours, MTT-product was stabilized with 40 µL of 10% SDS (75746, Sigma-Adrich) in 0.01 M HCl (76021889.2500, Boom). After 72 hour stabilization at 37°C, the absorbance was read at 570 and 720 nm by using the BMG LABTECH's SPECTROstar Nano Microplate reader (601-1696). Subsequently, the absorbance values at 720 nm were subtracted from the absorbance values at 570 nm. Data was analysed using GraphPad Prism 9.3.1 software and plotted as nonlinear regression line of best fit for 50% growth inhibitory concentration (IC_{50}) +/- standard error of the mean (SEM). IC_{50} values were then compared between the compounds.

2.4. High throughput screening

2.4.1. Compound library

Screening experiments and processing were performed by the high-throughput screening facility of the Princess Máxima Center. The high-throughput (HTS) drug library used contains 199 drugs, whereof 193 are dissolved in DMSO and stored at room temperature (rt) under nitrogen atmosphere. Four drugs (metformin, perifosine, carboplatin and oxaliplatin) are dissolved in Milli-Q (MQ) and one (cisplatin) is dissolved in a saline solution, which are stored at -20°C. Before the high-throughput

screen, the 384-well working plates (384LDV-Plates, Labcyte) containing the dissolved drugs are shaken (30 min at rt) and centrifuged (1 min at 1500 rpm). Subsequently, the working plates are surveyed with the Echo 550 dispenser to determine whether the amount of solution in the wells is sufficient to start the screen (minimal 2.5 µl) and the DMSO percentage is >80%.

2.4.2. High-throughput drug screen

For single and combination high-throughput screening, 40 µl of medium containing cells (cell densities, Table S3) were plated in a flat bottom 384-well tissue culture treated microplate (3764, Corning, NY) using a Multidrop Combi reagent dispenser (5840300, Thermo Scientific). Cells were allowed to attach overnight under standard culturing conditions. For the combination screens, CHLA90 cells were first treated with 62.8 nM (IC_{10}), 111 nM (IC_{20}) or 290 nM (IC_{50}) Pidnarulex. AMC772T2 cells were treated with with 25 nM (IC_{50}) Pidnarulex or 300 nM (IC_{50}) BMH-21 for 72 hours at standard culturing conditions. After this, the drug screen was performed with 10 microplates and the HTS library containing 199 drugs using the high-throughput screening facility (Beckman Coulter with a Biomek i7 Automated Workstation). Using the Echo 550 dispenser, 100 nL of the drugs (in DMSO or MQ, at different concentrations) was added to the wells containing the cells, to yield final concentrations of 0.1 nM, 1 nM, 10 nM, 100 nM, 1 µM and 10 µM (0.25% DMSO or MQ). Several drugs were tested at additional lower concentrations (up to 10 pM) or higher concentrations (up to 200 µM). Cells treated with only DMSO were used as positive controls, whereas cells treated with staurosporine (final concentration of 10 µM) were used as negative controls. The cells were incubated with the compounds for 72 hours at standard culturing conditions. Next, the MTT cell viability assay is performed. At the day of the drug screen, at t=0 hours, the MTT assay was also performed on one 384-well microplate containing untreated cells to eventually asses cell growth of untreated cells in wells in the beginning vs. the end of the screen (t=72).

2.4.3. MTT cell viability assay

5 µL of MTT solution (5 mg/mL MTT in sterile PBS) was added per well, and the microplates were incubated for 4 hours at standard culturing conditions. Next, 40 µL of 10% SDS/0.01 M HCl was added per well, and the microplates were incubated for 24-48 hours at standard culturing conditions. Subsequently, the absorbance at 570 nm and background absorbance at 720 nm was measured using the Spectramax i3x (molecular device). After this, the absorbance values at 720 nm were subtracted from the absorbance values at 570 nm, and the corresponding values were used to plot the dose-response curves.

2.4.4. Data processing

Finally, the half maximal concentration that inhibits the viability (IC_{50}) and area under the curve (AUC) were derived from the dose-response curves using the extension package drc in the statistic environment of R Studio (version 4.0.2). The data was normalized to the DMSO-treated cells (defined as 100% viability) and the empty controls (0% viability). IC_{50} values at 72 hours were calculated by determining the concentrations of the drug needed to achieve a 50% reduction in cell viability. AUC values were calculated by determining the definite integral of the curve. Quality of the screens was approved after assessment of the cell growth (absorbance signal of t72/t0), the negative, positive, and empty controls, and the amount of variability between the duplicates.

2.5. Western blotting

Protein lysates were prepared from cell pellets by scraping the cells with Leammli buffer (20% glycerol, 4% SDS, and 100mM Tris-HCl, pH 6.8 in MilliQ). The lysates were homogenized by hydrodynamic shearing through a 23G and 27G needle, followed by 10 min incubation at 50°C. Protein was quantified using the DC protein assay purchased from Bio-Rad (500112). Equal amounts of protein (12 µg) from

each cell lysate with 5X dithiothreitol (DTT) loading buffer were separated by sodium dodecyl sulfate polyacrylamide gel electrophoresis (SDS-PAGE) using 4-20% mini-protean TGX precast gels (4568096, Bio-Rad) and 1x Tris-Glycine-SDS running buffer. After running the gel, proteins were transferred to a polyvinylidene fluoride (PVDF) membrane with the Trans-Blot Turbo RTA Mini PVDF kit (1704272, Bio-Rad) using the Mixed MW protocol of the Trans-Blot Turbo Transfer System (1704150, Bio-Rad). The membrane was then blocked with 5% (w/v) ECL Prime blocking agent (RPN418V, Cytiva) in TBS/0.1% Tween (TBST) for 1 hour at rt and probed overnight with several primary antibodies (Table S2) at 4°C. Blots were washed 3 times for 5 min with TBST, incubated with the appropriate secondary antibody linked to horseradish peroxidase (HRP) for 1 hour at RT, and washed 4 times for 10 min before detection. All antibodies were diluted in 5% (w/v) ECL Prime blocking agent in TBST and all incubation steps described here should be performed in rotating falcon tubes on a roller. Antibody detection was accomplished using the ECL Select Detection Reagent (RPN2235, Cytvia) with exposure to ChemiDoc Imaging System (17001402, Bio-Rad) scanning for chemiluminescence. Exposure times vary widely, from a few seconds to 6 min, depending on the protein level strength.

3. Results

3.1. High-throughput screening to identify a selective compound for ATRX aberration neuroblastoma

To examine new therapy possibilities for patients with ATRX aberrations, ATRX wildtype and mutant human derived neuroblastoma have been selected as models for drug screens. The most common ATRX aberrations in neuroblastoma patients are in-frame deletions of whole exons. The ATRX gene locus consists of 35 exons and the exons 2 to 10 are most frequently deleted (Unpublished meta-analysis, van Gerven *et al*). Therefore, we performed drug screens with cell lines that also posses this deletion. AMC772T2 and SKNMM delete exon 2-9, but skip exon 10 and both show a 2-10 deletion on protein level (Figure 1S). The third most common ATRX exon deletion is 2-9, which is represented by CHLA90. We also selected four ATRX wildtype neuroblastoma cell lines (GIMEN, SY5Y, SJNB8 and NB139) that serve as controls. During the screen, cells were exposed 72 h to the HTS compound library containing six or more concentrations of 199 drugs, consisting of approved drugs used in cancer treatment and targeted compounds that are currently in (pre)clinical development for treatment. In these screens we did not find an ATRX specific overlapping hit in AMC772T2, CHLA90, and SKNMMM when compared to GIMEN, the wild type ATRX line (Figure S2, S4A, SKNMM data not shown). This finding could possibly be caused by the TP53 status of CHLA90 and SKNMM. TP53 is involved in cell-cycling arrest and apoptosis, and these cell lines are both TP53 mutated. Mutation of TP53 is found to reduce sensitivity to treatment in neuroblastoma[28], and therefore possibly did not result in an overlapping hit in all ATRX models. This data indicates that we were not able to identify a selective compound for ATRX aberration neuroblastoma out of the 199 compounds tested.

3.2. High-throughput screening identified drug resistance in ATRX del 2-10 neuroblastoma models

Previously in our lab isogenic ATRX aberrant models were established. These models were created in GIMEN, a Non-MYCN-amplified TP53 wildtype neuroblastoma line, to investigate whether the effect of the compounds tested is ATRX dependent. We performed high-throughput drug screening to identify fast implementable selective compounds against ATRX aberrant cell lines. In this screen, we used the isogenic wild-type (WT) and ATRX 2-10 (del 2-10) model lines. No selective compounds for $ATRX^{del\ 2\text{-}10}$ models were identified, however, we did observe resistance against multiple compounds (Figure 1A). Interestingly, four of these compounds (Nilotinib, Sorafenib, THZ531, Sepantronium bromide) are involved in inhibiting cell proliferation[29], and $ATRX^{del\ 2\text{-}10}$ cells grow substantially slower than the motherline. This slower growth could make them less sensitive to inhibition of cell proliferation. One of these compounds, Sepantronium bromide, even showed an average fold change of ~5 in IC_{50} value for $ATRX^{del\ 2\text{-}10}$ cells (Figure 1B, 1C). The isogenic ATRX models were used to exclude the effect of TP53 status on drug sensitivity in order to find an ATRX specific compound. However, we did not observed such ATRX dependent effect in this screen.

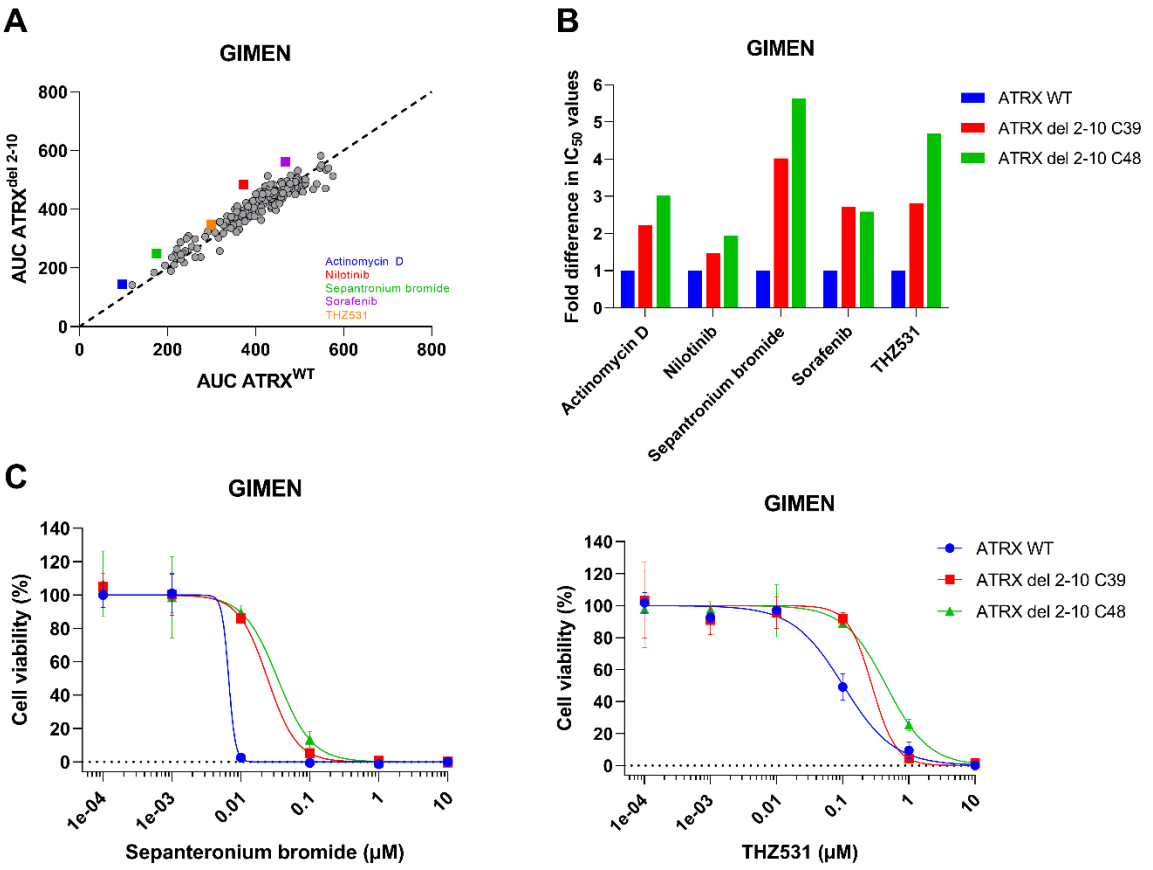

Figure 1 High-throughput screening identified drug resistance in ATRX del 2-10 neuroblastoma models. (A) Drug AUC values for ATRX^{WT} (X-axis) cells versus ATRX$^{del\ 2\text{-}10}$ clone 39 and clone 48 (Y-axis). For each compound, the area under the curve (AUC) values were calculated. Each dot represents a single compound. Coloured compounds above the diagonal line are less effective in the ATRX$^{del\ 2\text{-}10}$ cells. (B) Fold difference in IC_{50} values between ATRX^{WT} cells and ATRX$^{del\ 2\text{-}10}$ cells. Results are shown for the top 5 compounds showing the largest fold increase in IC_{50} value between the ATRX^{WT} cells and ATRX$^{del\ 2\text{-}10}$ cells. (C) Dose-response curves of 2 compounds with the largest fold increase in IC_{50} value, Sepantronium bromide and THZ531, in ATRX^{WT} and ATRX$^{del\ 2\text{-}10}$ cells. Dose-response curves represent the average (± SEM) result of a duplicate screen.

3.3. Chk1, RNA polymerase I, and WRN inhibition reduces cell viability in neuroblastoma patient-derived cell lines

Since no selective compounds could be identified through high-throughput screening, we selected compounds for a focused screen. From literature it is known that ATRX knockdown and deletions lead to increased G4s and replication fork stalling, which may lead to increased DNA damage[12]. Therefore, we suggested ATRX mutant cell lines to be more sensitive to inhibition of the pathway repairing these DNA damages, leading to even more DNA damage. Here, we selected 12 compounds consisting of DNA damaging agents (G4 stabilizers BMH-21, Pidnarulex, and Quarfloxin) and DNA damage repair inhibitors (WRNi; NSC 617145, BRCA1i; BRCA1-IN-2, RAD51i; RI-2, MRNi; Mirin, RESTi; X5050, RAD52i; D-I03, and BLMi; ML216). Cells were exposed 144 h to the compounds, after which the cell viability was measured. Subsequently, the AUC and IC_{50} values were calculated and assessed in order to identify the most effective compounds (Figure 2A, 2B). In addition, in a test screen with 72 h and 144 h treatment of Pidnarulex, we discovered that longer treatment of 144 h was more effective in almost all neuroblastoma lines tested (Figure 2C). We found a large shift in the curve with an IC_{50} fold change of ~10 in some cell lines when treated longer (Figure 2D).

While we did not find an ATRX specific compound, NSC 617145, Prexasertib, BMH-21, and Pidnarulex showed potential in reducing cell viability in all neuroblastoma lines after six days of treatment. Prexasertib inhibits Checkpoint kinase 1 (Chk1) and shows the most promising results in all cell lines, however, this effect is most possibly caused by deletion of 11q, which makes cells more sensitive for Chk1 inhibition. AMC772T2, CHLA90, and SKNMM are 11q deleted so we can not state whether the effect is 11q or ATRX-dependent. Therefore, we decided to focus on the other three identified effective compounds. AMC772T2 and GIMEN are most sensitive to treatment with Pidnarulex, NSC 617145 and Prexasertib. CHLA90 and SKNMM show the least response to almost all compounds tested. This observed pattern could be explained by the mutant TP53 status of these two cell lines, making them less responsive to therapy according to literature[30]. Again, no ATRX specific hits were identified after screening with selected compounds.

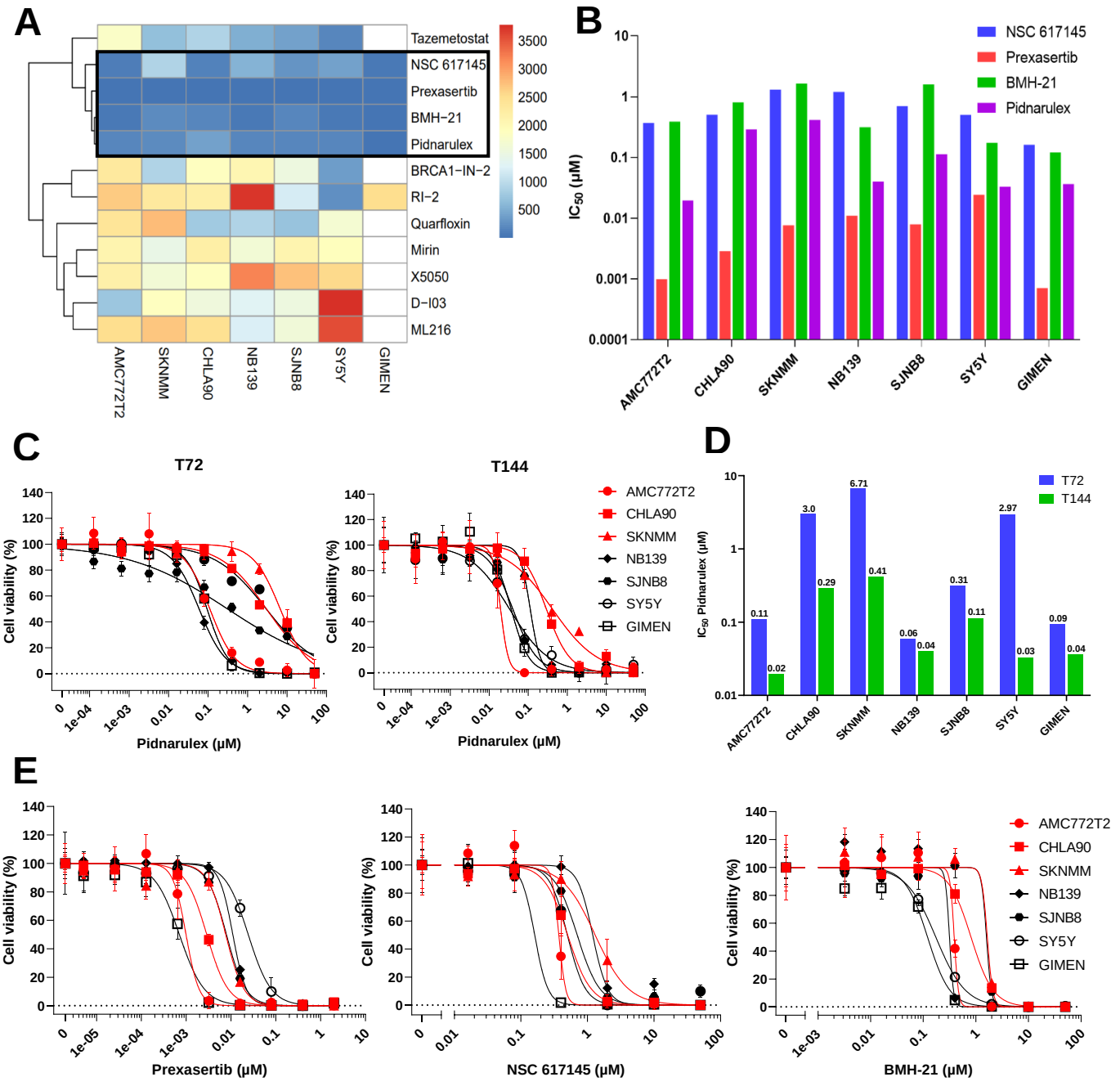

Figure 2 Chk1, RNA polymerase I, and WRN inhibition reduces cell viability in neuroblastoma patient-derived cell lines. (A) Heatmap of the AUC of the 12 compounds that were tested *in vitro*. The four most effective compounds are highlighted in black. (B) Bar graph showing the IC_{50} values of the four selected compounds after 6 days of treatment. (C) Dose-response curve of Pidnarulex (RNA polymerase Ii) after 3 and 6 days of treatment, ATRX mutant models are indicated in red. (D) Bar graph showing the IC_{50} values of Pidnarulex after 3 and 6 days of treatment. (E) Dose-response curves of NSC 617145 (WRNi), Prexasertib (Chk1i), and BMH-21 (RNA polymerase Ii) after a treatment period of 6 days. ATRX mutant lines are shown in red.

3.4. The effect of RNA polymerase I and WRN inhibition is not specific for isogenic ATRX neuroblastoma cell lines

Furthermore, we wanted to investigate if the three most potent compounds found in patient derived neuroblastoma lines were ATRX specific, independently of TP53 mutations. Therefore, we performed a second screen on selected isogenic GIMEN models in which the only deviation is ATRX status. One of these developed models has an ATRX exon 2-13 deletion, which is the largest in-frame exon deletion found in ATRX neuroblastoma patients and still results in an ATRX IFF protein product. In the other models used for screening, ATRX was knocked out (KO) or ATRX exon 2 to 10 was deleted, the most common in-frame deletion in patients (Figure S3, Meta-analysis, van Gerven *et al.*). For all three compounds tested, only limited differences were observed in IC_{50} values between the ATRX mutants and ATRX wild type models. The curves plotted show no preferential sensitivity of the compounds for ATRX mutant lines (Figure 3). Taken together, these *in vitro* results indicate that treating ATRX WT and ATRX mutant neuroblastoma cells with NSC 617145, BMH-21 or Pidnarulex is effective in inducing an apoptotic response. Unfortunately, none of these therapies led to significant differences in sensitivity between the ATRX WT and ATRX mutant models. From this we can conclude that NSC 617145, BMH-21 and Pidnarulex are not ATRX specific.

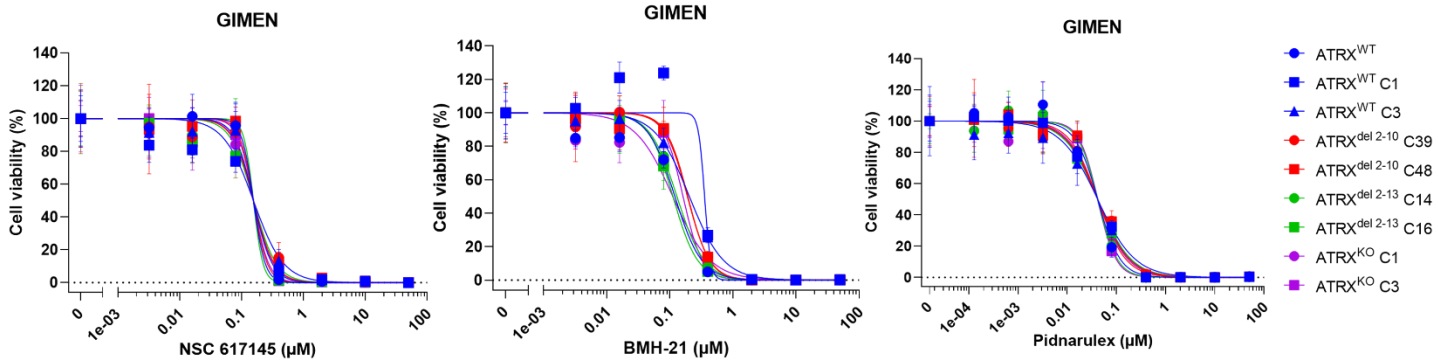

Figure 3 The effect of RNA polymerase I and WRN inhibition is not specific for isogenic ATRX neuroblastoma cell lines. Dose-response curves of NSC 617145, BMH-21 and Pidnarulex after six days of treatment in GIMEN isogenic models. The blue curves represent GIMEN ATRX WT clones, red curves indicate ATRX 2-10 deletion clones, green curves show drug responses in ATRX 2-13 deletion clones, and purple lines indicate ATRX KO clones.

3.5. Pidnarulex and BMH-21 probably do not show synergy in a high-throughput combination screen

Combination therapies are a successful strategy to enhance efficacy in cancer, so therefore we decided to combine Pidnarulex and BMH-21 with other compounds to find an additive or synergistic effect. Two ATRX neuroblastoma models, AMC772T2 and CHLA90, were incubated with primary compound (Pindarulex or BMH-21) for 72 hours, followed by another 72 hour incubation with the HTS library (199 compounds). AMC772T2 cells did not receive the whole HTS library due to an error in the robot and therefore only 167 compounds (32 missing compounds) were added and tested for synergy. Judging from the dose-response curves, AUC and IC_{50} values of the monotherapy and combination therapy (Figure 4, S4B, S4C), we did not observe synergy in any of the drug pairs examined. Additionally, we tested the 12 selected compounds for synergy (Table S4). However, also no synergy was observed in these drug combination screens. Together, these results demonstrate that both Pidnarulex and BMH-21 alone kill AMC772T2 and CHLA90 efficiently. However, combination therapy with these drugs has not shown potential to become a very promising high-risk neuroblastoma therapy so far.

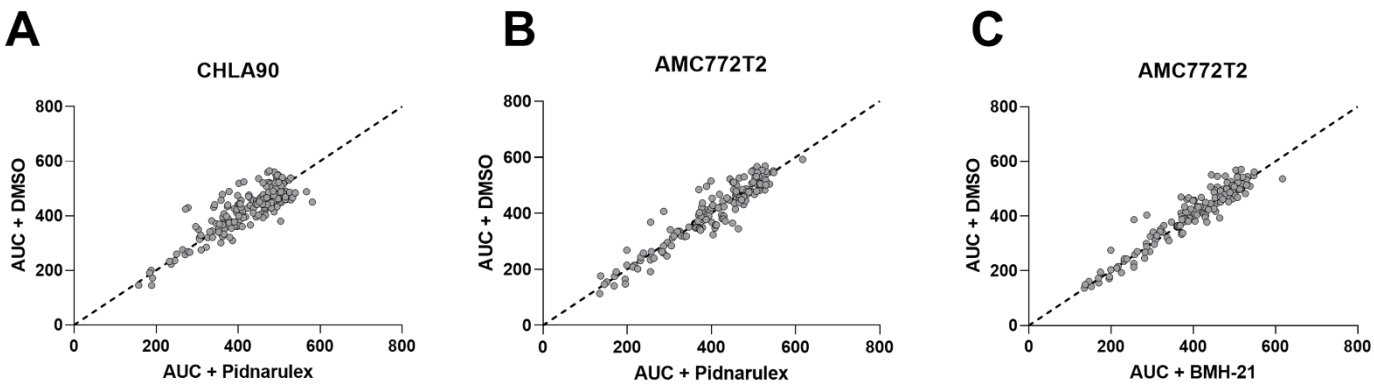

Figure 4 Pidnarulex and BMH-21 probably do not show synergy in high-throughput combination screen. For each compound, the AUC values were calculated. Each dot represents a single compound. Compounds underneath the diagonal line are more effective in combination than as monotherapy. (A) Drug AUC values for CHLA90 + Pidnarulex in combination with the whole HTS library (199 compounds, X-axis) versus CHLA90 + Pidnarulex (Y-axis). (B, C) Drug AUC values for AMC772T2 + Pidnarulex/BMH-21 in combination with the HTS library (167 compounds) versus AMC772T2 + Pidnarulex/BMH-21 (Y-axis).

4. Discussion

Available therapy options for children with high-risk neuroblastoma are limited, a problem that must be overcome to improve the prognosis of these children. Our study aimed to identify new effective therapies for ATRX aberrant neuroblastoma tumours to increase the overall survival rate for high-risk neuroblastoma. Here, we performed single and combination drug screens on patient-derived neuroblastoma cell lines and isogenic ATRX neuroblastoma models. While over 200 compounds were tested in this study, we were not able to identify a specific hit for ATRX. However, we found five compounds that are less sensitive for treatment in isogenic GIMEN ATRX del 2-10 models. Also, inhibitors of G4/RNA polymerase I (Pol I; Pidnarulex and BMH-21), Werner syndrome RecQ like helicase (WRN; NSC 617145), and Chk1 (Prexasertib) were identified and shown to be effective in all neuroblastoma lines.

In this study, we revealed that isogenic ATRX$^{del\ 2\text{-}10}$ models are less affected by a few compounds of the HTS library. Our drug screen showed resistance to these compounds in ATRX$^{del\ 2\text{-}10}$ models when compared to ATRX^{WT} models. Most of these identified compounds are cytostatics, and therefore involved in inhibiting cell proliferation[29]. ATRX$^{del\ 2\text{-}10}$ models grow substantially slower in culture than the motherline and cytostatics effectively target rapidly-dividing cells[31], which could make them less sensitive to therapy with cytostatics. Also, two compounds (Nilotinib and Sorafenib) that were found to be less effective in ATRX$^{del\ 2\text{-}10}$ both function in inhibiting tyrosine kinases and are clinically used to treat leukaemia, kidney and liver cancer[32,33]. Interestingly, previously in our lab, we did not demonstrate such resistance in ATRX^{KO} cells compared to ATRX^{WT} cells. This indicates that the effect we see is probably ATRX$^{del\ 2\text{-}10}$ specific. However, no therapy resistance was found in ATRX$^{del\ 2\text{-}10}$ models when treated with other cytostatics of the HTS library. These cytostatics include doxorubicin and cisplatin that are currently being used in the clinic to treat neuroblastoma, and drugs that are in (pre)clinical development. Taken together, these findings need further validation in order to investigate their mechanism of resistance.

Prexasertib, the inhibitor of CHk1, was found to be the best hit in our screens. Our three ATRX mutant neuroblastoma lines (AMC772T2, CHLA90, and SKNMM) were all more sensitive to treatment than three out of four ATRX WT neuroblastoma lines. AMC772T2, CHLA90, SKNMM, and GIMEN are 11q deleted, and Keller *et al* (Unpublished paper Kaylee Keller) have linked Prexasertib sensitivity to 11q status. They observed that 11q deleted neuroblastoma cell lines are more sensitive to Chk1 inhibition with a lower IC_{50} value in the 11q deleted cell lines than the 11q wild-type cell lines. Therefore, we suspect the sensitivity found in our patient derived neuroblastoma cell lines to be more related to 11q status than to ATRX status. In our isogenic GIMEN ATRX models we did not observe preferential sensitivity for ATRX mutants, independently of 11q status. Therefore, we can confirm that ATRX aberrations do not increase sensitivity for Prexasertib.

During the last decade, G4 structures became of interest as a therapeutic target due to their roles in regulating DNA replication, gene expression, telomere protection, and genome stability[34]. ATRX is thought to resolve those structures, and ATRX loss is linked to replication stress[35]. Pidnarulex and Quarfloxin are inhibitors that are structurally related and suggested to have G4 stabilizing activities[36]. Wang *et al* found Quarfloxin and Pidnarulex to selectively induce cell death in ATRX mutant glioma patient-derived stem cells and in ATRX deficient isogenic glioma models[37]. However, in our data, Quarfloxin was not found to be effective in either of the neuroblastoma cell lines. Moreover, Pidnarulex was effective in all of the neuroblastoma cell lines. This effectiveness might be explained by the finding that Pidnarulex also inhibits ribosomal RNA (rDNA)[38].

It has been observed that ATRX binds rDNA repeats[39] and Pol I transcribes rDNA to rRNA, which is essential for ribosomal biogenesis and genome stability[40]. Loss of ATRX is linked to rDNA instability and decreased rRNA transcription by Pol I in mouse embryonic stem (ES) cells[41]. Therefore, inhibiting Pol I at rDNA loci is suggested to specifically kill cancer cells that are ATRX-mutated[41]. Pidnarulex and BMH-21 are such Pol I inhibitors that were tested for ATRX specificity in our neuroblastoma lines[38,42]. Both inhibitors were shown to be effective, however, no increased sensitivity in ATRX-mutant and KO models was found. This contradicts findings in the literature, showing that mouse ES ATRX KO cells are more sensitive to Pidnarulex treatment when compared to ATRX WT cells[41]. In addition, it is not certain if Pidnarulex is a specific RNA polymerase I inhibitor. Recent studies found that Pidnarulex stabilizes G4 complexes[36] or primarily inhibits topoisomerase II beta (TOP2B)[43] in tumours. Pan *et al* also found TOP2B expression to be similar among different neuroblastoma cell lines and tumours[43]. This finding may explain why Pidnarulex is not ATRX specific in our data. Pidnarulex effectiveness has also been tested in other cancers including leukaemia, lymphoma, and sarcoma[44,45]. In a database, 912 cell lines were screened for Pidnarulex and the lowest IC_{50} value was found in leukemia cells (0.06 µM)[46], while we found IC_{50} values of Pidnarulex ranging from 0.02 to 0.41 µM in our neuroblastoma lines. When comparing these IC_{50} values between other cancers, neuroblastoma is quite sensitive to treatment with Pidnarulex[46]. This indicates that Pidnarulex may be of interest for neuroblastoma therapy in general. In addition, BMH-21 was also found to be linked to TOP2B inhibition[47]. In a study they observed that BMH-21's target is a binding partner of TOP2A and TOP2B in the nucleolus[47]. Therefore, it is suggested that BMH-21 also indirectly inhibits TOP2B, which may explain the effectiveness of this compound in neuroblastoma cell lines.

The other compound that was shown to be effective in neuroblastoma lines is the WRN inhibitor NSC 617145. WRN functions in the DDR and is suggested to be involved in resolving G4 structures[48]. ATRX-mutated lines are predicted to have more G4 structures and DNA damage, which would make them more sensitive for inhibition of members of the DDR. However, we did not observe increased sensitivity for NSC 617145 in our ATRX models. In a study , this compound was found to effectively kill T-cell leukemia cells with an IC_{50} ranging from 0.013 to 0.32 µM[49]. When comparing the IC_{50} values found in our neuroblastoma cell lines (0.29 to 1.31 µM), we suggest that NSC 617145 is more effective in leukaemia cells. However, the sensitivity for WRN inhibition in all neuroblastoma lines can possibly be explained by the function of progerin, a truncated version of the lamin A protein[50]. In a study it was found that WRN naturally inhibits progerin[51] and in another study they found progerin able drive neuroblastoma cells into senescence[52]. Theoretically, inhibiting WRN would therefore result in more progerin, leading to increased cell cycle arrest and decreased proliferation of neuroblastoma cells. This proposed mechanism of action might clarify the effectiveness of NSC 617145 in our neuroblastoma models. NSC 617145 was not tested in combination and since it was shown to be an effective inhibitor in all neuroblastoma lines tested, finding a synergistic combination could be possible.

Finally, we performed combination screens for Pidnarulex and BMH-21, but due to an error in the robot, 32 compounds available were not tested for synergy. Because some compounds were missing in the combination screens, it is recommended to repeat these screens in the future. Unfortunately, we did not find a specific ATRX hit in the single and combination screens. Despite these limitations in our data, our results suggest that we found three compounds for neuroblastoma cells in general. Pidnarulex, BMH-21, and NSC 617145 are not specific for ATRX, but are of interest for future research. In the future, it is recommended to perform a CRISPR-Cas9 screen in order to possibly identify a specific target for ATRX neuroblastoma.

References

1. Colon, N. C. & Chung, D. H. Neuroblastoma. *Adv. Pediatr.* **58**, 297 (2011).
2. Esiashvili, N., Anderson, C. & Katzenstein, H. M. Neuroblastoma. *Curr. Probl. Cancer* **33**, 333–360 (2009).
3. Stiller, C. A. & Parkin, D. M. International variations in the incidence of neuroblastoma. *Int. J. Cancer* **52**, 538–543 (1992).
4. Jansky, S. *et al.* Single-cell transcriptomic analyses provide insights into the developmental origins of neuroblastoma. *Nat. Genet. 2021 535* **53**, 683–693 (2021).
5. Lonergan, G. J., Schwab, C. M., Suarez, E. S. & Carlson, C. L. From the archives of the AFIP - Neuroblastoma, ganglioneuroblastoma, and ganglioneuroma: Radiologic-pathologic correlation. *Radiographics* **22**, 911–934 (2002).
6. Moreno, M. M., Barrell, W. B., Godwin, A., Guille, M. & Liu, K. J. Anaplastic lymphoma kinase (alk), a neuroblastoma associated gene, is expressed in neural crest domains during embryonic development of Xenopus. *Gene Expr. Patterns* **40**, 119183 (2021).
7. Ngan, E. S. W. Heterogeneity of neuroblastoma. *Oncoscience* **2**, 837 (2015).
8. Sbeih, A. H., Salami, K., Morabito, F. & Saleh, H. Epidemiological and Clinical Data in Low and Intermediate Risk Neuroblastoma: A Single Institution Experience and Survival Outcomes in Jerusalem. *Asian Pacific J. Cancer Care* **5**, 139–144 (2020).
9. Smith, V. & Foster, J. High-Risk Neuroblastoma Treatment Review. *Children* **5**, (2018).
10. Valentijn, L. J. *et al.* TERT rearrangements are frequent in neuroblastoma and identify aggressive tumors. *Nat. Genet. 2015 4712* **47**, 1411–1414 (2015).
11. Cheung, N. K. V. *et al.* Association of age at diagnosis and genetic mutations in patients with neuroblastoma. *JAMA* **307**, 1062–1071 (2012).
12. Zeineldin, M. *et al.* MYCN amplification and ATRX mutations are incompatible in neuroblastoma. *Nat. Commun.* **11**, (2020).
13. George, S. L. *et al.* Therapeutic vulnerabilities in the DNA damage response for the treatment of ATRX mutant neuroblastoma. *EBioMedicine* **59**, (2020).
14. Qadeer, Z. A. *et al.* ATRX In-Frame Fusion Neuroblastoma Is Sensitive to EZH2 Inhibition via Modulation of Neuronal Gene Signatures. *Cancer Cell* **36**, 512–527 (2019).
15. Picketts, D. J. *et al.* ATRX encodes a novel member of the SNF2 family of proteins: mutations point to a common mechanism underlying the ATR-X syndrome. *Hum. Mol. Genet.* **5**, 1899–1907 (1996).
16. Nandakumar, P., Mansouri, A. & Das, S. The role of ATRX in glioma biology. *Front. Oncol.* **7**, 236 (2017).
17. Pekmezci, M. *et al.* Adult infiltrating gliomas with WHO 2016 integrated diagnosis: additional prognostic roles of ATRX and TERT. *Acta Neuropathol.* **133**, 1001–1016 (2017).
18. Law, M. J. *et al.* ATR-X Syndrome Protein Targets Tandem Repeats and Influences Allele-Specific Expression in a Size-Dependent Manner. doi:10.1016/j.cell.2010.09.023.
19. Wang, Y. *et al.* G-quadruplex DNA drives genomic instability and represents a targetable molecular abnormality in ATRX-deficient malignant glioma. *Nat. Commun.* **10**, (2019).

20. Rhodes, D. & Lipps, H. J. G-quadruplexes and their regulatory roles in biology. *Nucleic Acids Res.* **43**, 8627–8637 (2015).

21. Técher, H., Koundrioukoff, S., Nicolas, A. & Debatisse, M. The impact of replication stress on replication dynamics and DNA damage in vertebrate cells. *Nat. Rev. Genet.* **18**, 535–550 (2017).

22. Garbarino, J., Eckroate, J., Sundaram, R. K., Jensen, R. B. & Bindra, R. S. Loss of ATRX confers DNA repair defects and PARP inhibitor sensitivity. *Transl. Oncol.* **14**, (2021).

23. Leung, J. W. C. *et al.* Alpha thalassemia/mental retardation syndrome X-linked gene product ATRX is required for proper replication restart and cellular resistance to replication stress. *J. Biol. Chem.* **288**, 6342–6350 (2013).

24. Voon, H. P. J., Collas, P. & Wong, L. H. Compromised Telomeric Heterochromatin Promotes ALTernative Lengthening of Telomeres. *Trends in cancer* **2**, 114–116 (2016).

25. Garbarino, J., Eckroate, J., Sundaram, R. K., Jensen, R. B. & Bindra, R. S. Loss of ATRX confers DNA repair defects and PARP inhibitor sensitivity. *Transl. Oncol.* **14**, 101147 (2021).

26. Liang, J. *et al.* Genome-Wide CRISPR-Cas9 Screen Reveals Selective Vulnerability of ATRX-Mutant Cancers to WEE1 Inhibition. *Cancer Res.* **80**, 510–523 (2020).

27. Han, B. *et al.* Loss of ATRX suppresses ATM dependent DNA damage repair by modulating H3K9me3 to enhance temozolomide sensitivity in glioma. *Cancer Lett.* **419**, 280–290 (2018).

28. Xue, C. *et al.* p53 determines multidrug sensitivity of childhood neuroblastoma. *Cancer Res.* **67**, 10351–10360 (2007).

29. Ziogas, I. A. & Tsoulfas, G. Evolving role of Sorafenib in the management of hepatocellular carcinoma. *World J. Clin. Oncol.* **8**, 203 (2017).

30. Tchelebi, L., Ashamalla, H. & Graves, P. R. Mutant p53 and the response to chemotherapy and radiation. *Subcell. Biochem.* **85**, 133–159 (2014).

31. Pérez-Herrero, E. & Fernández-Medarde, A. Advanced targeted therapies in cancer: Drug nanocarriers, the future of chemotherapy. *Eur. J. Pharm. Biopharm.* **93**, 52–79 (2015).

32. Blay, J. Y. & Von Mehren, M. Nilotinib: a Novel, Selective Tyrosine Kinase Inhibitor. *Semin. Oncol.* **38**, S3 (2011).

33. Hasskarl, J. Sorafenib: targeting multiple tyrosine kinases in cancer. *Recent Results Cancer Res.* **201**, 145–164 (2014).

34. Awadasseid, A., Ma, X., Wu, Y. & Zhang, W. G-quadruplex stabilization via small-molecules as a potential anti-cancer strategy. *Biomed. Pharmacother.* **139**, 111550 (2021).

35. Teng, Y. C. *et al.* ATRX promotes heterochromatin formation to protect cells from G-quadruplex DNA-mediated stress. *Nat. Commun. 2021 121* **12**, 1–14 (2021).

36. Xu, H. *et al.* CX-5461 is a DNA G-quadruplex stabilizer with selective lethality in BRCA1/2 deficient tumours. *Nat. Commun. 2017 81* **8**, 1–18 (2017).

37. Wang, Y. *et al.* EXTH-34. G-QUADRUPLEX DNA DRIVES GENOMIC INSTABILITY AND REPRESENTS A TARGETABLE MOLECULAR ABNORMALITY IN ATRX-DEFICIENT MALIGNANT GLIOMA. *Neuro. Oncol.* **20**, vi92 (2018).

38. Haddach, M. *et al.* Discovery of CX-5461, the First Direct and Selective Inhibitor of RNA Polymerase I, for Cancer Therapeutics. *ACS Med. Chem. Lett.* **3**, 602–606 (2012).

39. Ren, W. *et al.* Disruption of ATRX-RNA interactions uncovers roles in ATRX localization and PRC2 function. *Nat. Commun. 2020 111* **11**, 1–15 (2020).

40. Laferté, A. *et al.* The transcriptional activity of RNA polymerase I is a key determinant for the level of all ribosome components. *Genes Dev.* **20**, 2030–2040 (2006).

41. Udugama, M. *et al.* Ribosomal DNA copy loss and repeat instability in ATRX-mutated cancers. *Proc. Natl. Acad. Sci. U. S. A.* **115**, 4737–4742 (2018).

42. Jacobs, R. Q., Huffines, A. K., Laiho, M. & Schneider, D. A. The small-molecule BMH-21 directly inhibits transcription elongation and DNA occupancy of RNA polymerase I in vivo and in vitro. *J. Biol. Chem.* **298**, 101450 (2022).

43. Pan, M. *et al.* The chemotherapeutic CX-5461 primarily targets TOP2B and exhibits selective activity in high-risk neuroblastoma. *Nat. Commun. 2021 121* **12**, 1–20 (2021).

44. Khot, A. *et al.* First-in-Human RNA Polymerase I Transcription Inhibitor CX-5461 in Patients with Advanced Hematologic Cancers: Results of a Phase I Dose-Escalation Study. *Cancer Discov.* **9**, 1036–1049 (2019).

45. Negi, S. S. & Brown, P. rRNA synthesis inhibitor, CX-5461, activates ATM/ATR pathway in acute lymphoblastic leukemia, arrests cells in G2 phase and induces apoptosis. *Oncotarget* **6**, 18094–18104 (2015).

46. Drug: CX-5461 - Cancerrxgene - Genomics of Drug Sensitivity in Cancer. https://www.cancerrxgene.org/compound/CX-5461/300/overview/ic50.

47. Morotomi-Yano, K. & Yano, K. ichi. Nucleolar translocation of human DNA topoisomerase II by ATP depletion and its disruption by the RNA polymerase I inhibitor BMH-21. *Sci. Rep.* **11**, (2021).

48. Mendoza, O., Bourdoncle, A., Boulé, J. B., Brosh, R. M. & Mergny, J. L. G-quadruplexes and helicases. *Nucleic Acids Res.* **44**, 1989 (2016).

49. Moles, R., Bai, X. T., Chaib-Mezrag, H. & Nicot, C. WRN-targeted therapy using inhibitors NSC 19630 and NSC 617145 induce apoptosis in HTLV-1-transformed adult T-cell leukemia cells. *J. Hematol. Oncol.* **9**, 1–11 (2016).

50. Kaminski, A., Fedorchak, G. R. & Lammerding, J. The cellular mastermind(?) - Mechanotransduction and the nucleus. *Prog. Mol. Biol. Transl. Sci.* **126**, 157–203 (2014).

51. Kang, S. mi *et al.* Human WRN is an intrinsic inhibitor of progerin, abnormal splicing product of lamin A. *Sci. Reports 2021 111* **11**, 1–14 (2021).

52. Bahmad, H. F. *et al.* Cancer stem cells in neuroblastoma: Expanding the therapeutic frontier. *Front. Mol. Neurosci.* **12**, 131 (2019).

Supplementary data

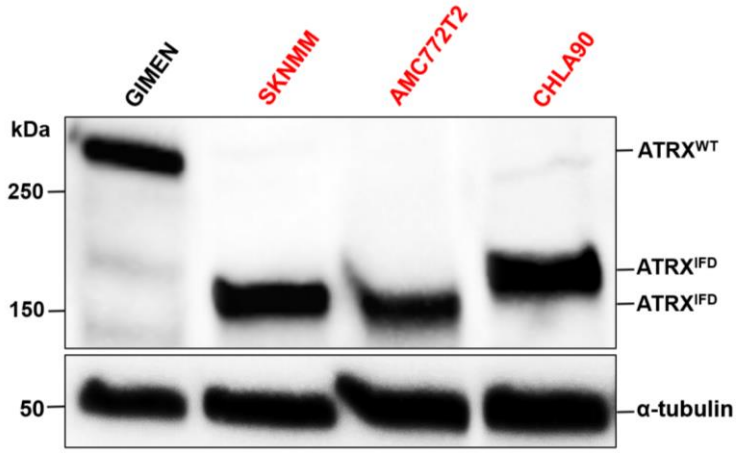

Figure S1: Western blot analysis of ATRX wild type (WT) and ATRX in-frame deletion (IFD) protein product in neuroblastoma models. The ATRX mutant lines are indicated in red.

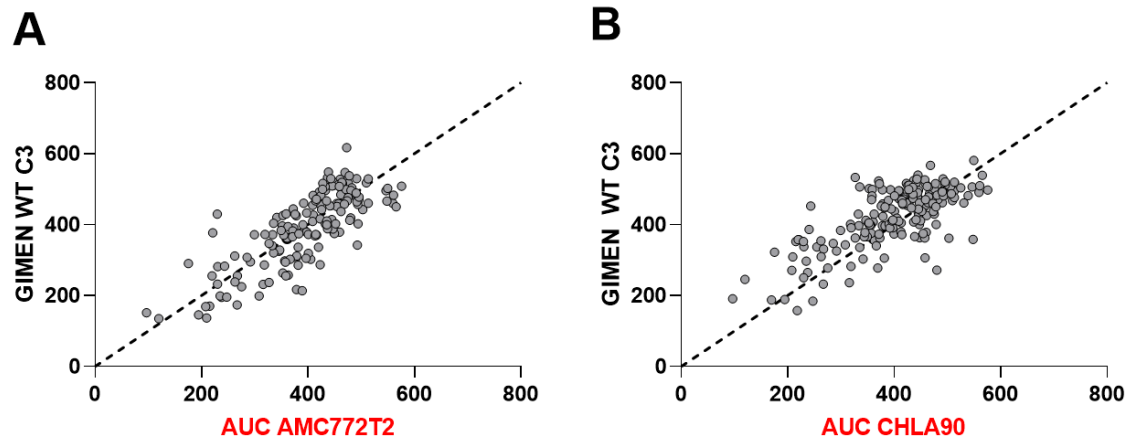

Figure S2: High-throughput screening to identify a selective compound for ATRX aberration. (A) Drug AUC values for AMC772T2 (X-axis) cells versus ATRX$^{del\ 2\text{-}10}$ clone 39 and clone 48 (Y-axis). Each dot represents a single compound. Compounds above the diagonal line are less effective in the ATRX$^{del\ 2\text{-}10}$ cells.

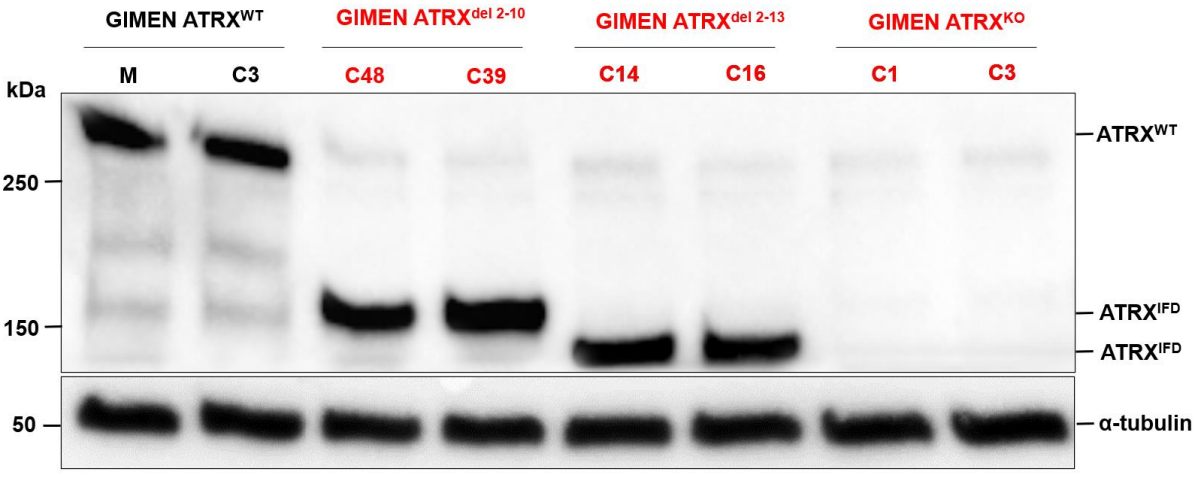

Figure S3: ATRX Western blot of isogenic GIMEN models. The ATRX mutant lines are indicated in red. ATRX protein size shows the in-frame-deletion (IFD) protein product of the incorporated exon deletions.

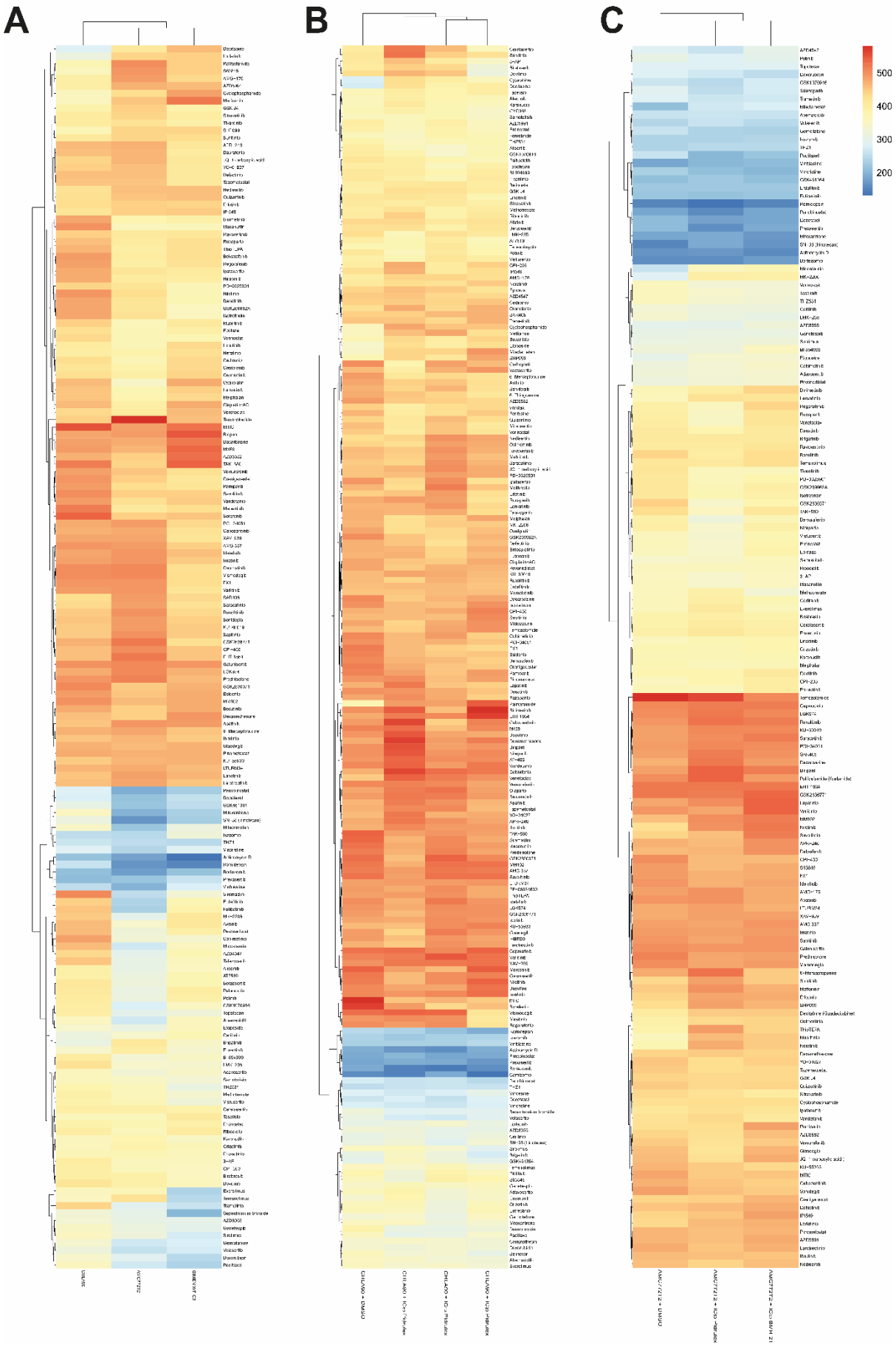

Figure S4 Heatmaps of the single and combination high throughput screens. (A) AUC of single compound test with the HTS library containing 199 compounds on AMC772T2, CHLA90, and GIMEN WT C3. (B) AUC of screen with Pidnarulex IC_{10}, IC_{20}, and IC_{50} concentration in combination with the HTS library on CHLA90. (C) AUC of screen with Pidnarulex and BMH-21 IC_{50} concentration in combination with the HTS library on AMC772T2.

Table S1: Cell lines and culture media used.

Cell line/Organoid	Main medium components	Supplements
AMC772T2	Dulbecco's Modified Eagle's Medium (DMEM) low glucose + GlutaMAX containing 1 g/L D-glucose and pyruvate (21885025, Gibco, Thermo Fisher)	20% Ham's F-12 Nutrient Mix + GlutaMAX (31765027, Gibco, Thermo Fisher), 1% Penicillin/Streptomycin (P/S, 15140122, Gibco, Thermo Fisher), B-27 without vitamin A (50X, 12587010, Gibco, Thermo Fisher), N2 supplement (100X) (17502048, Gibco, Thermo Fisher), 0.2 µg/ml Epithelial Growth Factor (hEGF), 0.4 µg/ml Fibroblast Growth Factor basic (hFGF), 2 µg/ml human Insulin-like Growth Factor 1 (hIGF1), and 0.1 µg/ml human Platelet Derived Growth Factor (PDGF) AA and BB.
CHLA90	Iscove's Modified Dulbecco's Medium (IMDM) containing L-glutamine and 25 mM HEPES (12440053, Gibco, Thermo Fisher)	10% Fetal Bovine Serum (FBS) (F0804, Sigma-Aldrich), 1% P/S, Insulin Transferrin Selenium (100X) (ITS, 41400045, Gibco, Thermo Fisher), and 2 mM L-glutamine (25030024, Gibco, Thermo Fisher).
GIMEN/GIMEN clones, SJNB8, SKNSH, and SY5Y	DMEM containing 4.5 g/L D-glucose, and L-glutamine (41965039, Gibco, Thermo Fisher)	10% FBS, 1% P/S, 2 mM L-glutamine, and 1% MEM Non-Essential Amino Acids Solution (100X) (NEAA, 11140035, Gibco, Thermo Fisher).
NB139	DMEM low glucose + GlutaMAX containing 1 g/L D-glucose and pyruvate (21885025, Gibco, Thermo Fisher)	20% Ham's F12 Nutrient Mix, 1% P/S, B-27 without vitamin A (50X), 0.2 µg/ml Epithelial Growth Factor (hEGF), and 0.4 µg/ml Fibroblast Growth Factor basic (hFGF).
SKNMM	Roswell Park Memorial Institute (RPMI) 1640 medium containing L-glutamine (21875059, Gibco, Thermo Fisher)	10% FBS and 1% P/S.

Table S2: Antibodies used for Western blotting.

Target	Antibody type	Dilution	Supplier
ATRX	Rabbit pAb, IgG	1:500	Abcam (ab97508)
COX-IV	Rabbit mAb, IgG	1:2000	Abcam (ab202554)
HA-tag	Rabbit mAb, IgG	1:250	Cell Signaling (C29F4)
Histone H3.3	Rabbit pAb, IgG	1:500	Merck Millipore (09-838)
mH2A1	Rabbit pAb, IgG	1:1000	Abcam (ab37264)
α-tubulin	Mouse mAb, IgG	1:10,000	Cell Signaling (DM1A)
γH2A.X	Rabbit pAb, IgG	1:500	Abcam (ab2893)
Mouse IgG	Sheep IgG-HRP	1:5000	Amersham ECL GE Healthcare (NXA931V)
Rabbit IgG	Donkey IgG-HRP	1:5000	Amersham ECL GE Healthcare (NA9340V)

Table S3: Seeding densities used in drug screens per cell line.

Cell line/organoid	Seeding density t72 (cells/well) in 384 well plate	Seeding density t144 (cells/well) in 384 well plate
AMC772T2	3000	1500
CHLA90	3800	1200
GIMEN	800	200
GIMEN WT clones	1500	500
GIMEN 2-10 del clones	1500	300
GIMEN 2-13 del clones	800	150
GIMEN KO clones	1200	200
NB139	800	1200
SJNB8	1800	1200
SKNMM	1400	700
SY5Y	5000	3500

Table S4: Compound combinations tested in AMC772T2.

Compound 1	Compound 2	Additive/synergistic effect? Y/N
Pidnarulex	ML216	N
Pidnarulex	Tazemetostat	N
Pidnarulex	Quarfloxin	N
Pidnarulex	Mirin	N
Pidnarulex	RI-2	N
Pidnarulex	D-I03	N
Pidnarulex	X5050	N
Pidnarulex	NSC 617145	N
Pidnarulex	Prexasertib	N
Pidnarulex	BCRA1-IN-2	N
Mirin	BRCA1-IN-2	N
Mirin	ML216	N
Mirin	RI-2	N
Mirin	D-I03	N
Mirin	NSC 617145	N
BRCA1-IN-2	RI-2	N
BRCA1-IN-2	D-I03	N
BRCA1-IN-2	ML216	N
BRCA1-IN-2	NSC 617145	N
RI-2	D-I03	N
RI-2	ML216	N
RI-2	NSC 617145	N
D-I03	ML216	N
D-I03	NSC 617145	N
ML216	NSC 617145	N